Refereed Proceedings

The 13th International Conference on Fluidization - New Paradigm in Fluidization Engineering

Engineering Conferences International *Year* 2010

BIOMASS GASIFICATION IN ROTATING FLUIDIZED BED

Mania Abdollahi* Christophe Guy†

Jamal Chaouki‡

*Ecole Polytecnique Montreal, mania.abdollahineisiani@polymtl.ca

†École Polytechnique

‡École Polytechnique

BIOMASS GASIFICATION IN ROTATING FLUIDIZED BED

Mania Abdollahi-Neisiani, Christophe Guy and Jamal Chaouki

Chemical Engineering Department, École Polytechnique, Montréal H3C 3A7, Canada

Abstract

A steady-state mathematical model is developed for a rotating fluidized bed gasifier. Integrating reactor hydrodynamics with devolatilization kinetics, char gasification and combustion of both char and gas species; the model is used to present the gas-solid phenomena in novel reactor and investigates the reactor application in gasification processes. Model outputs are compared with experimental and simulation results of existing fluidized bed gasifier. It is observed that for the same equivalence ratio, the gasification process in RFB-SG is improved as a result of improved heat and mass transfer and gas-solid contact.

1. Introduction

The conversion of biomass into useful forms of energy and chemicals can be achieved in a number of ways. However the conversion of biomass to combustible gas through gasification is considered as one of the promising options for biomass conversion and utilization [1]. Due to the presence of numerous endothermic and exothermic reactions in the gasification mechanism, it is necessary to maintain a high heat transfer throughout the reactor. This requirement makes fluidized bed reactors favorable for gasification process. Fluidized bed reactors had been used and studied extensively for the biomass gasification process. A fluidized bed provides two important features to the gasification process: a medium in which rapid heating of the biomass particle can take place and, by adding an inert medium to the bed, a controlled fluidization environment and uniform temperature over a wide range of biomass feed rates. In conventional fluidized bed gasifiers, carrier gas flows vertically upward through a bed of fine particles. The upward flow forms a fluidized particle zone with velocities ranging from minimum fluidization to particle elutriation velocity. Fluidized bed heat and mass transfer rates are governed by the Reynolds Number, as well as velocities and residence times of particles in the bed. Increasing the velocity decreases the solid hold up in the bed region resulting in reduction of gas-solid mixing in that area. It may also decrease particle residence time in the bed causing particles to elutriate prior to reaction. These issues can be overcome by fluidizing through the reactor walls using a *rotating* fluidized bed rather than the conventional vertical gas injection. The concept of rotating fluidized beds first was introduced in 1978, applications and improvements followed over the years [2]. In older rotating designs, fluidization gas was injected *radially* through the outer wall of reactor and the particles were fluidized against an outward centrifugal force created by the rotation of the reactor wall. The rotational motion of the reactor caused several operational problems like vibration, complicated sealing and difficulty in solid feeding and removal. A new RFB design overcomes these difficulties while benefiting from centrifugal forces. In the rotating fluidized bed-static geometry (RFB-SG) recently developed [3, 4], fluidizing gas enters *tangentially* inward to the fluidization chamber via multiple gas inlet slots at the outer cylindrical wall. As a result of the tangential gas-solid drag force, solid particles in the fluidization chamber rotate and experience a radially-outward centrifugal force (figure 1). In the radial direction, the gas-solid drag force is opposite to the centrifugal force. The

centrifugal force is determined by the rotational speed of the particle bed and can be a multiple of Earth gravity. This leads to vertical and horizontal operation, significantly higher fluidization gas velocity, and increased gas-solid radial slip velocity. These phenomena increase heat and mass transfer and minimize the elutriation of particles so that both small and large particles are reacted. One of the most features of RFB-SG is high solid hold up in the bed region despite the very high gas velocities. This leads to much improved solid-gas mixing in the reactor compared to fluidized bed reactors for processes such as gasification. To evaluate these claims and investigate the potential of the RFB-SG, the biomass gasification process is simulated in this type of reactor and the final product yield and process intensification were compared with the fluidized bed gasifier.

2. Theoretical concept of model

Comprehensive modeling of any reactor requires a good knowledge of chemical reaction kinetics and reactor hydrodynamics. Kinetic part describes most important chemical changes that take place in the reactor, while hydrodynamics account for transport processes. Integration of kinetics and hydrodynamics provide comprehensive description of gasifier processes and performances.

2.1 Kinetic models

The following reactions will include in the gasification model:

A. *Pyrolysis:* upon entering the hot sand particle zone of the gasifier, biomass particles undergo pyrolysis. Pyrolysis is the decomposition of biomass structure because of heat in the absence of oxygen. Total devolatilization, which determines the extent of produced char and individual gas release, is considered in the kinetic model. The kinetic model, used for important products (H_2, CO, CO_2, CH_4, tar and char), is a single first order reaction and can be described by the following equation:

$$\boldsymbol{dV_i/dt = k_{0,i} e^{\left(-E_i/RT\right)} (V_i^* - V_i)} \qquad (1)$$

Where V_i and V_i^* are the instantaneous and total amounts of volatile matter for the gaseous component presented as i. The kinetic model (Eq.1) used for this model was proposed by Nunn et al. [5] for wood at high heating rates (1000 K/s). The parameters used for kinetic of pyrolysis were summarized in table 1.

B. *Secondary pyrolysis or tar cracking:* Thermal decomposition of tar is another important step in kinetic expressions because more that 60% of pyrolysis products contain tar. This reaction takes place in the gas phase. Boroson et al. [6] proposed a first order reaction for the tar-cracking step. The same model is also used in this study; its parameters are shown in table 2.

Tar cracking reaction:

$$tar\ (gas) \rightarrow \vartheta_{H_2} H_2(g) + \vartheta_{CH_4} CH_4(g) + \vartheta_{CO} CO(gas) + \vartheta_{CO_2} CO_2(gas) + \vartheta_{tar} tar_{inert}$$

And the kinetic model is as follows:

$$\boldsymbol{r_{cracking} = \vartheta_i 10^{4.98} exp\left(\frac{-9210}{RT}\right) \rho_{tar}} \qquad \boldsymbol{\frac{kg}{kg.s}} \qquad (2)$$

Where ρ_{tar} is the amount of tar in the gas phase and ϑ_i .is the stoichiometric coefficient as presented in table 13.

C. *Tar combustion:* tar, like char and other combustible materials is subject to combustion in the reactor. The kinetic model of Brydon et al. was used for this group of reactions [7].

$$CH_{1.522}O_{0.0228} + 0.867\ O_2 \rightarrow CO + 0.761\ H_2O$$

And reaction rate is expressed as :

$$r = 9.2 \times 10^6 T \exp(\frac{-9650}{T})[tar]^{0.5}[O_2]\ \text{, kmol/m3.s} \quad (3)$$

D. Homogenous and heterogeneous reactions: table 4 shows other *important* reactions taking place in the reactor.

Table 1, kinetic parameters for primary pyrolysis [5]

Component	Log (k_{0i}) [1/s]	E_i [kcal/mol]	V_i* [kg/kg biomass]
Total devolatilization	4.53	16.5	92
Total gas	2.38	11.8	41
H_2	6.7	27	2
CH_4	3.79	16.6	3.6
CO	3.36	14.6	17.0
CO_2	3.77	14.3	6.0
H_2O	3.35	11.5	5.14
Char= 100- (total devolatilization)			
Tar= (total devolatilization)-(total gas release)			

Table 2, Stoichiometric coefficients for tar cracking [6]

Component	ϑ_i
H_2	0.0173316
CH_4	0.0884052
CO	0.563316
CO_2	0.1109316
Secondary tar	0.22

2.2 Mathematical description of the RFB-SG model

In gasification reactors, biomass particles undergo fast pyrolysis following their entrance into the high-temperature zone. Hence, solid particles in the bed also include char and ash. In this model, only char particles undergo reactions while ash particles are considered inert. Here, hydrodynamics of the solid particles and of the flowing gas are different. So it is necessary to define two separate reactors: one for the gas and one for the solid phase. For the sake of simplicity reacting particles are assumed to be diluted (no interaction) and possible heat exchange between the particles and the walls of the reactor will be ignored. Based on primary observations of the RFB-SG [3], this reactor was modeled at a specific operation condition where there is sufficient solids in the bed so that no bubble formation is observed. Operation conditions and reactor specifics are presented in table 3. The RFB-SG model assumes that the gas form each inlet; undergoes a number of different plug

flow regimes (in radial direction) without any interaction between them. The gases freshly formed by pyrolysis of particles enter some of the plug flow reactors and mix with fluidization gas (air). A mixture of un-reacted and reacted vapors leaves each reactor and enters to the volume near the chimney where they mix with the fresh air entered from other inlets and all the vapors eventually exit. However char particles produced form biomass pyrolysis experience different flow patterns compared to gas-phase. Upon entering the reactor, a tangential gas momentum is transferred to the solid particles, where they experience a rotational motion. Here, in the case of char flow pattern an ideal plug flow reactor and perfectly mixed reactor (in *tangential* direction) are considered. As a result the solid is modeled in the two extremes of contacting pattern. Gas velocities at each of inlet are assumed to be equal. This assumption may not be correct because of some non-uniformity in solid distribution. The following equations

Table 3, Assumed operating condition and reactor dimensions (RFB-SG and BFB)

		units	value
Operating condition	Particle material		Sand
	Average particle size	m	300×10^{6}
	Solid loading in RFB-SG	kg	1.5
	Total gas flow rate in RFB-SG	m^3/s	0.2
	Temperature	°C	800
	ER	-	Same for two reactors
Reactor specifications (RFB-SG)	Number of gas inlet slots	-	12
	Slots width	mm	4
	Reactor outer diameter	m	0.36
	Reactor inner diameter (chimney)	m	0.15
	Reactor length	m	0.135
	Radial gas velocity at gas inlet	m/s	2.6
Reactor specifications (FB)	Reactor diameter	mm	78
	Reactor length	m	0.75
	Air velocity	m/s	0.1

present the mass balance for the gas phase in the *radial* direction and for char particles in the *tangential* phase. The overall presentation of the model is shown in figure2.

- Gas phase:

$$\frac{d(F_{i,r})}{dV_{g,r}} + \sum_{g-g} \upsilon_{ij} R_i + \sum_{g-s} \upsilon_{ij} R_i = 0 \qquad (4)$$

- Solid phase:

$$\frac{d(F_{c,\theta})}{dV_{c,\theta}} + \sum_{g-s} \upsilon_{ij} R_i = 0 \qquad (5)$$

$$F_{c,\theta} - F_{c,0} + V \sum_{g-s} \upsilon_{ij} R_i = 0$$

As it was observed by De Wild *et. al.* there exists a region near the chimney exit where solid hold-up is much lower compared to regions close to outer walls, which is called the freeboard [3] and is limited to homogeneous reactions only. In the RFB-SG reactor the gas from all inlets enter the region before existing from chimney outlet. The gas flow in this region was considered as a plug-flow. The Mass balance equation for gas species in the freeboard is expressed as the follows:

Table 4. List of homogenous and heterogeneous reactions involved in gasifiers

Chemical reaction	Kinetic	Ref.
Heterogeneous reactions (1/s)		
$2\left(\frac{\eta+1}{\eta+2}\right) C + O_2 \rightarrow \frac{2\eta}{\eta+2} CO + \frac{2}{\eta+2} CO_2$	$\frac{dX}{dt} = 5.3 \times 10^5 \exp(\frac{-125000}{RT_{par}}) P_{O_2}^{0.53}(1 - X_{c)}{}^{0.49}$ $\eta = 2500\exp(-\frac{6240}{T_{par}})$	[8]
$C + H_2O \rightarrow CO + H_2$	$\frac{dX}{dt} = 1.23 \times 10^7 \exp\left(-\frac{198000}{RT_{par}}\right) P_{H_2O}(1 - X)$	[9]
$C + CO_2 \rightarrow 2CO$	$\frac{dX}{dt} = \frac{9.1 \times 10^6}{T^{0.8}} \exp\left(-\frac{166000}{RT_{par}}\right) P_{CO_2}{}^{0.8}(1 - X)^{2/3}$	[10]
Homogenous reactions		
$CO + H_2O \leftrightarrow H_2 + CO_2$	$r = k\left([CO][H_2O] - \frac{[CO_2][H_2]}{K}\right); K = 0.0265 \exp\left(\frac{3958}{T}\right)$	[11]
$H_2 + \frac{1}{2} O_2 \rightarrow H_2O$	$r = k\,[O_2][H_2]^{1.5}; (\frac{mol}{m^3.s}).; k = 1.631 \times 10^9\, T^{1.5} \exp\left(\frac{-3420}{T}\right)$	[12]
$CO + \frac{1}{2} O_2 \rightarrow CO_2$	$r = k\,[CO][O_2]^{0.25}[H_2O]^{0.5};\ (\frac{mol}{m^3.s})$	[13]
$CH_4 + 2\ O_2 \rightarrow CO_2 + 2H_2O$	$r = k\,[CH_4]^{0.7}[O_2]^{0.8}; \left(\frac{mol}{m^3.s}\right); k = 1.6 \times 10^{10} \exp(-\frac{24157}{T})$	[13]

Plug-flow mass balance for gas species in freeboard region:

$$\frac{d(F_{i,fb})}{dV_{fb}} + \sum_{g-g} \upsilon_{ij} R_i = 0 \qquad (6)$$

Where $F_{i,b}$ is the gas species flow rate exiting from the bed section, obtained from solving Eq.4 and R_i is the reaction rate for homogeneous and heterogeneous reactions presented in table 4. Reactor dimensions and operating conditions are summarized in table 3. Gas product compositions, obtained from solving these equations, are compared with values calculated from fluidized bed reactor model.

2.3 Mathematical description of the fluidized bed model

A one-dimensional two-phase model is used to describe gasification in bubbling fluidized bed gasifier (BFBG). The bed is divided into a particle-lean bubble phase surrounded by the particle-rich emulsion phase with mass transfer occurring between these two phases. Mass balance for the gas-phase in the bubble and emulsion phases could be written as following:

- ***Bubble phase:***

$$-\delta_b \frac{d(C_{i,b}u_b)}{dz} + K_{be}(C_{i,e} - C_{i,b}) + \delta_b(1-\gamma_b)\sum_{g-g}\upsilon_{ij}R_i + \delta_b\gamma_b\sum_{g-s}\upsilon_{ij}R_i = 0 \qquad (7)$$

- ***Emulsion phase:***

$$-(1-\delta_b)\varepsilon_{mf}\frac{d(C_{i,e}u_{mf})}{dz} + K_{be}(C_{i,b} - C_{i,e}) + \varepsilon_{mf}(1-\delta_b)\sum_{g-g}\upsilon_{ij}R_i + (1-\delta_b)(1-\varepsilon_{mf})\sum_{g-s}\upsilon_{ij}R_i = 0 \quad (8)$$

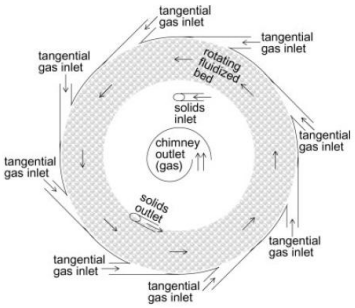

Figure 1. Schematic of the rotating fluidized bed in a static fluidization chamber [3]

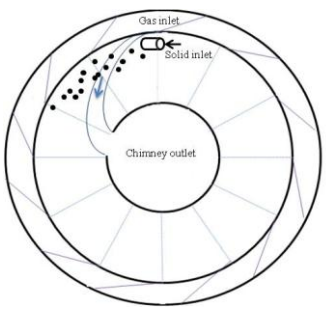

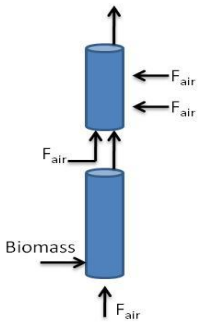

Figure 2. Overall presentation of the RFB-SG model and model domain

Equations 9 and 10 describes the gas concentration profile for each species in the bed. The characteristics of the fluidzed bed reactor used for the this model is presented in table 3. Hydrodynamic parameters for fluidized bed (δ_b, u_b, K_{be},ε_{mf},etc) were calculated based on information proposed by Radmanesh et al.[14].

3. Results and Discussion

Biomass gasification is modeled in both a bubbling fluidized bed gasifier (section 2.3) and Rotating fluidized bed gasifier (section 2.2). Simulation results from both gasifiers were compared. Outputs were also compared to experimental data from bottom biomass feeding in fluidized bed reactor.

In feeding from the bottom, pyrolysis products pass through the bed and there is better mixing of the gas products. The char particles also go under combustion reactions (heterogeneous reactions), where their products (CO and CO_2) mix with the pyrolysis gases and other products resulting from homogenous reactions. The concentration of gas products in the bed region is calculated by solving Eqs. (4, 5) and in the freeboard region by solving Eqs. (6 or 7) at specific operating condition (ER=0.26). Boundary conditions for the mass balance equations are given by the pyrolysis kinetic model listed in table 1, which gives the composition of the gas components, tar and char at biomass feeding point [5]. Product compositions from gasification in RFB-SG are compared with the results from gasification in bubbling fluidized bed at the same equivalence ratio (ER). ER is an important parameter in air-blown biomass gasification. It is defined as the air-to-fuel mass flow ratio used in the experiment divided by the air-to-fuel mass flow ratio required for a complete combustion. Table 5 summarizes the assumed operating conditions in each reactor

and the resulting gas-phase product composition. For comparison, the experimental results reported by Narvaez *et al* were used [15].

Table 5. Gasification product gas composition in dry basis, fluidized bed reactor and rotating fluidized bed

Reactor	Model summary	T_{bed} (°C)	ER	High Heating Value (MJ/Nm^3)	Gas composition at exit (Dry Basis %)				
					H_2	CH_4	CO	CO_2	N_2
Rotating Fluidized bed (single biomass inlet)	Bed: *PFR* Freeboard: *PFR* Solid: *CSTR*	800	0.26	4.6	1.2	3.5	22.7	4.1	69.0
	Bed: *PFR* Freeboard: *PFR* Solid: *PFR*			3.5	1.8	4.2	12.6	2.7	78.7
Rotating Fluidized bed (multiple biomass inlet)	Bed: *PFR* Freeboard: *PFR* Solid: *PFR*			5.1	12.7	3.5	16.5	2.1	65.0
Fluidized bed (*experiments*) [15]	-			4.0	9.4	3.2	12.4	15.0	60.0
Fluidized bed (*model*)	Two-phase model			4.4	11.2	3.4	12.7	13.9	58.8

In the case of RFB-SG gasification, it is assumed that biomass enters the reactor close to gas inlet slots. As it was discussed in section 2.2, the produced gas biomass pyrolysis go through gasification and combustion reactions, then the products will meet with fresh air entered form other gas inlets in the freeboard region. This phenomenon in mixing of gas products is one of the disadvantages of the current design of RFB-SG, because as it is also obtained from the model results (table 5), the produced H_2 from gasification reactions will combust before exiting form the chimney, resulting in lower H_2 production compared with Fluidized bed reactors. However as in table 5 yields of CO from the RFB are favorably higher than yields from the BFBG. Operating at higher ER, the yield of hydrogen decreased probably as a result of hydrogen combustion. The yield of CO_2 is lower in RFB-SG compared to BFBG. The high heating value (HHV) of any kind of fuel is defined as the amount of heat released by a specified quantity (initially at 25 C) once it is combusted and the products have returned to a temperature of 25°C. The high heating value (HHV) of the dry gas produced form gasification process at the standard state can be estimated by the following equation [16]:

$$\boldsymbol{HHV} = \frac{(\mathbf{12.75}[\boldsymbol{H_2}]+\mathbf{12.63}[\boldsymbol{CO}]+\mathbf{39.82}[\boldsymbol{CH_4}])}{\mathbf{100}} \ \boldsymbol{MJ}/\boldsymbol{Nm^3} \qquad (9)$$

The HHV estimated from equation 9, for product gas from RFB-SG and BFB gasifiers is also listed in table 5. It could be observed that with the current design, RFB-SG gasifier produces gas with close value of HHV compared to BFBG. The HHV in both reactors decreased by increasing of ER due to larger contributions of CO_2 and lower contribution of CO and H_2 in the yield of gas products. As forecasted by the RFB-SG model, char particles were consumed after a very short residence time and mixing of the produced gas from gasification reactions with air from other gas inlets results in H_2 yield reduction. Consequently an alternative approach for increasing process efficiency in RFB-SG is to add more solid inlets in the reactor.

Practically, the system becomes single vessel containing multiple reactors with all reaction products mixing in the region near the chimney outlet which will enhance the gas yield per reactor volume. The results for the multiple solid inlets are listed in table 5 where the operating condition and reactor characteristics are kept the same as shown in table 3. In the concept of multiple solid inlets in RFB-SG, the oxygen presence in the fluidization agent will be consumed in partial combustion of char and other combustible gases presence in the pyrolysis products and will be consumed completely before entering in the freeboard region. Therefore the final produced gas from RFB-SG has higher H_2 and CO and lower CO_2 content compared to the BFBG. RFB-SG shows strong potentials in gasification applications. Successful industrial application of RFB for gasification processes requires better understanding of the gas- and solid-phase hydrodynamics to develop more comprehensive models.

4. Conclusion

RFB-SG exhibit excellent particle mixing and heat transfer properties resulting in higher solid hold up in the bed area compared with the conventional fluidized reactors. A steady-state mathematical model was presented of a rotating fluidized bed gasifier which integrates reactor hydrodynamics with the devolatilization kinetics, char gasification and combustion of char and gas species. Model outputs confirm the potential of rotating fluidized beds in static geometry for improving syngas yields. Further investigations on RFB-SG hydrodynamics are required.

REFERENCES

1. McKendry, P., *Energy production from biomass (part 2): conversion technologies.* Bioresource Technology 2002. **83**(1): p. 47-54.
2. O'Connor, C., *Rotating fluidized bed combustor*. 1978.
3. De-Wilde, J. and A. De-Broqueville, *Rotating fluidized beds in a static geometry: Experimental proof of concept.* AIChE Journal, 2007. **53**(4): p. 793 - 810.
4. De-Wilde, J. and A. de-Broqueville, *Experimental Study of Fluidization of 1G-Geldart D-Type Particles in a Rotating Fluidized Bed with a Rotating Chimney.* AIChE Journal, 2008. **54**(8): p. 2029-2044.
5. Nunn, T.R., et al., *Product compositions and kinetics in the rapid pyrolysis of sweet gum hardwood.* Ind Eng Chem Proc Des Dev, 1985. **24**: p. 836-844.
6. Boroson, M.L., et al., *Product yields and kinetics from the vapor phase cracking of wood pyrolysis tars.* AIChE 1987. **35**(1): p. 120 - 128.
7. Bryden, K.M. and K.W. Ragland, *Numerical Modeling of a Deep, Fixed Bed Combustor.* Energy Fuels, 1996. **10**(2): p. 269-275.
8. Janse, A.M.C., et al., *Combustion Kinetics of Char Obtained by Flash Pyrolysis of Pine Wood.* Ind. Eng. Chem. Res., 1998. **37**(10): p. 3909-3918.
9. Hemati, M. and C. Laguerie, *Détermination de la cinétique de vapogazéification de charbon de bois en thermobalance.* Entropie 1988. **142**: p. 29-40.
10. VanDenAarsen, F., A. Beenackers, and W.V. Swaaij, *Wood pyrolysis and carbon dioxide char gasification kinetics in a fluidized bed*. Fundamentals of biomass thermochemical conversion. 1985: London: Elsevier.
11. Parent, J.D. and S. Katz, *Equilibrium Compositions and Enthalpy Changes for the Reaction of Carbon, Oxygen, and Steam.* IGT-Inst. Gas Tech., Research Bulletin 2, 1948.
12. Jensen, A., et al., *Formation and reduction of NOx in pressurized fluidized bed combustion of coal.* Fuel, 1995. **74**(11): p. 1555-1569.
13. Souza-Santos, M.L.d., *Solid fuels combustion and gasification : modeling, simulation, and equipment operation*. 2004.
14. Radmanesh, R., J. Chaouki, and C. Guy, *Biomass Gasification in a Bubbling Fluidized Bed Reactor: Experiments and Modeling.* AIChE, 2006. **52**(12).
15. Narvaez, I., et al., *Biomass gasification with air in an atmospheric bubbling fluidized bed. Effect of six operational variables on the quality of the produced rawgas.* Ind.Eng. Chem.Res., 1996. **35**(7): p. 2110-2120.
16. Lia, X.T., et al., *Biomass gasification in a circulating fuidized bed.* Biomass and Bioenergy, 2004. **26**: p. 171 - 193.